Influence of reaction time, temperature and heavy metal on characteristics of cellulose- and wood-derived hydrochars from hydrothermal carbonization

Xin Zhao
FZJ: Forschungszentrum Julich GmbH
Jin Huang (huangj@caf.ac.cn)
Chinese Academy of Forestry
Zhaonan Li
Huazhong University of Science and Technology
Yao Chen
Tianjin University
Michael Müller
FZJ: Forschungszentrum Julich GmbH

Research Article

Keywords: Cellulose, Wood, HTC, Hydrochars, Lignite-like fuel, Heavy metal

Posted Date: April 7th, 2022

DOI: https://doi.org/10.21203/rs.3.rs-851829/v2

Abstract

Hydrothermal carbonization (HTC) is a promising technique to convert biomass into valuable solid fuels. In this work, cellulose and wood-derived hydrochars were synthesized under hydrothermal carbonization conditions with different temperatures (200–250 ℃), reaction times (6 h or 12 h) and to determine their influence on hydrochars. Heavy metal element zinc is chosen to introduce into samples to simulate the heavy metal accumulate in biomass. The physical, chemical, and combustion properties of the hydrochars revealed that the majority of cellulose and wood conversion occurs at first 6 h, and faster conversion occurs at higher temperatures. The content of fixed carbon in the cellulose-derived hydrochar is higher than in wood-derived hydrochar. Moreover, cellulose is easier to be carbonized during HTC reaction than wood. O/C and H/C ratios of all hydrochars were similar to those of lignite and decreased with increasing reaction temperature. The composition of solids recovered after 12 h is similar at all temperatures, consisting primarily of sp^2 carbons (furanic and aromatic groups) and alkyl groups. When a large amount of metal is introduced, part of the metal is combined with the energetic group, while the rest condense on the surface of the sample as zinc ions.

Statement Of Novelty

There is limited knowledge studied the format of heavy metals in wood- and cellulose-derived hydrochar during the HTC process and the release behavior of heavy metals under high temperatures. In this work, the heavy metal element zinc is chosen to introduce into samples to simulate the heavy metal accumulate in biomass. And the impact of the reaction time, temperature, and heavy metal on characteristics of productions are systematically investigated.

1. Introduction

In broad terms, biomass can be defined as a complex that contains all livings, dead creatures, and their waste[1]. Biomass can be used as carbonaceous material, which is the feedback of fossil fuel resources such as coal, lignite, etc. Currently, biomass contributes to 10–14% of total energy consumption in the world [2]. Moreover, biomass-derived fuels have the potential to solve the global energy crisis and alleviate environmental pollution caused by the combustion of traditional fossil fuels [3]. Therefore, biomass has been considered as one of the most promising materials to replace non-renewable energy.

Several ways for biomass conversion toward valuable fuels such as pyrolysis, the biological conversion process, and HTC (hydrothermal carbonization) have been developed [4]. However, pyrolysis is not suitable for high moisture biomass waste because it needs high temperatures [5, 6]. The biological conversion processes, including fermentation and anaerobic digestion, are economical but at the expense of conversion time [5, 7]. The HTC process is carried out under mild conditions, avoiding the use of unsafe conditions such as high temperature and high pressure [8]. HTC process includes reactions such as hydrolysis, dehydration, decarboxylation, aromatization, and re-condensation [9]. And similar to pyrolysis, the HTC process, generated hydrochars characterized by high carbon, high energy, low

hydrogen, and oxygen [1, 8]. The emission of gases such as nitrogen oxides and sulfur oxides in water as acids or salts can be avoided during the HTC process [10]. HTC process has a low poisonous impact on materials, uses facile instrumentation and techniques, and effectively produces high energy and economy [11, 12]. Therefore, it is a suitable process for using biomass, even with high moisture contents that come from agricultural residues, wood, and herbaceous energy crops. In this respect, HTC has become an essential option for converting biomass to energy resources[13, 14].

Many experiments have reported that the hydrochars obtained by HTC can simulate the different low-rank coals [15, 16, 25, 17–24]. The temperature [26], reaction time [27], and pH [28] have different effects on the characteristics of hydrochar obtained by the HTC process. Also, the source of raw materials is an important factor that influences hydrochar properties. Numerous studies have mentioned hydrothermal carbonization of a variety of feedstocks such as bamboo [29], manure [30], sewage sludge [31], and municipal solid waste [32].

Because of urbanization, industrialization, and growth in pollution [32], the number of heavy metals is increased in biomass. Chemical, sewage sludge is a mixture of various organic and inorganic compounds. Several other elements, including heavy metals, are present in a variable content which are converted in the gaseous compounds during gasification [33]. The problem of pollutions in biomass hinders the process of biomass conversion, it is also significant to study it.

As a relatively simple feedstock, cellulose and wood were also used in HTC [27, 34–38]. However, to our best knowledge, the influence of the reaction time, temperature and heavy metals on the characteristics of hydrochars produced from cellulose and wood was not systematically investigated. This work aims to investigate the effect of residence time and temperatures on the physical, chemical, and combustion characteristics of the hydrochars produced from cellulose and wood via the HTC process, also compare the difference between cellulose-derived hydrochar and wood-derived hydrochar. This research can provide insight into the carbonization of cellulosic biomass and real biomass.

The characteristics of the obtained hydrochars were measured by using atomic absorption spectroscopy (AAS), thermogravimetry (TG-DTG), Fourier transform infrared spectrometry (FTIR), scanning electron microscope (SEM), thermogravimetric analysis (TGA), and X-ray photoelectron spectroscopy (XPS), molecular beam mass spectrometer (MBMS).

2. Materials And Methods

2.1. Materials

Pure α-cellulose was purchased from Alfa Aesar. A-quality wood pellets were delivered by the Labee Group in Moerdijk. The pellets were chopped into pieces (< 0.54 mm) using an IKA laboratory mill.

2.2. Experimental procedure

10 g of sample were suspended into a 1L Teflon-lined stainless-steel autoclave. 50 ml of deionized water was added into the reactor, heated in a vertical oven at 200 or 250 ◦C. The autoclave was transferred to an ambient temperature environment after 6 h or 12 h reaction time. The solid residue was washed with deionized water and filtered several times until the pH value was neutral, and then dried at a temperature of 100 ◦C in an oven for 12 h.

2.3. Characterization

The content of inorganic elements was measured via AAS. TGA measurement was performed to determine combustion behavior. A magnetic suspension balance with an online mass spectrometer was used to measure the weight loss under combustion conditions at the temperature ranging from room temperature to 800 ℃ in an air atmosphere (20% O2/N2) heating rate of 10 ℃/min. SEM images were acquired on Zeiss SUPRA 50VP instrument to investigate the physical morphology of hydrochars. The functional groups' information of the samples was investigated by FTIR (Nicolet 6700 FTIR) with a diamond ATR accessory and a resolution of 2 cm^{-1} from 4000 to 500. In terms of XPS analysis (Specs spectrometer), the binding energy of C 1s and O 1s were 284.82 eV and 532.75 eV, respectively.

3. Results And Discussion

3.1. Combustion behaviors analysis

Weight loss and rate of weight loss measurements are illustrated in Fig. 1, and the percentages of weight loss during the HTC reaction are shown in Table 1.

Table 1: Weight loss during three stages and residues of samples

Samples	Stage 1	Stage 2	Stage 3
C-200-6	3.4%	78.0%	8.5%
C-250-6	3.3%	39.9%	41.5%
C-250-12	2.6%	38.6%	41.7%
W-200-6	3.9%	65.3%	30.1%
W-250-6	2.6%	30.3%	54.7%
W-250-12	2.1%	25.4%	60.5%
C : Cellulose, W : Wood			

The first stage of TG-DTG (ambient to 100 ℃) is for the evaporation of moisture. Changes of TG-DTG are similar at the first stage, indicating a similar content of moisture in cellulose- and wood-derived. A plateau between 110 and 190 ℃ follows, where heating of molecules occurs without breaking chemical bonds.

The second stage is the combustion phase (200 - 400 ℃), including devolatilization and combustion of volatile matters (e.g., moisture and small organic molecules) and sample combustion [39]. Wood-derived hydrochar and cellulose-derived hydrochar obtained by HTC reaction at 200 ℃ lost most of the weight during the second stage. Wood- and cellulose-derived hydrochars obtained at 200 ℃ lost more weight than at 250 ℃. Moreover, at the same HTC condition, the weight loss of cellulose-derived hydrochars is higher than that of wood-derived hydrochar. It indicates these hydrochars obtained at 200 ℃ are mainly made of volatile matters, and the content of volatile matters in cellulose-derived hydrochar is higher than that of wood-derived hydrochar.

The third stage, i.e., the burn-out stage (450–550 ℃), is for the combustion of fixed carbon remaining after the preceding stages [40, 41]. Compared with the weight loss of hydrochars obtained at 250 ℃ in the third stage, the weight loss of hydrochars obtained at 200 ℃ is lower. That means more fixed carbon formed at 250 ℃. At the same HTC reaction condition, the wood-derived hydrochar lost more weight than cellulose-derived hydrochar. It indicates the content of fixed carbon in wood-derived hydrochars is higher than that in cellulose-derived hydrochars. When HTC reaction temperature is 250 ℃, the weight loss of the cellulose-derived hydrochars obtained at 6 h is similar to that of 12 h, meaning that fixed carbon does not change much with the increasing of time. While wood-derived hydrochar obtained in 12 h has significantly higher weight loss than that of 6 h. It means prolonging the reaction improves the content of fixed carbon for wood-derived hydrochar.

3.2. Structural properties of the hydrochars

Figure 2 and Fig. 3 are the SEM images of cellulose-derived and wood-derived hydrochar. Because of the incomplete hydrothermal reaction, an irregular shape is shown in the SEM image of cellulose-derived (Fig. 2a) and wood-derived (Fig. 3a) hydrochar produced at 200 ℃ and 6 h reaction time. Hydrochars have a compact structure without any pores proves cellulose and wood dissolve incompletely due to the low temperature of the HTC reaction. The microspheres formed on the surface of hydrochars because sectional cellulose was solubilized and/or hydrolyzed. These nano/microspheres were also generated by the decomposition of amorphous cellulose [42].

As shown in Fig. 2b and Fig. 3b, with 250 ℃ reaction temperature and 6 h reaction time, the surface of hydrochar became rougher as some pores and different sizes of small carbon microspheres were formed on the surface. One possible reason is that higher temperature facilitates the degree of solubility and/or hydrolysis of cellulose.

However, unlike cellulose-derived hydrochar, the microspheres formed on the surface of wood-derived hydrochar should be expected due to the conversion of hemicellulose, which is a fundamental component of wood [10]. The amount of sphere-like nano/microparticles of wood hydrochar is lower than that of cellulose-derived hydrochar under the same experimental conditions. It indicates that cellulose-derived hydrochar is much easier to be carbonized and/or hydrolyzed than wood-derived hydrochar.

It is illustrated in Fig. 2 (c-d) and Fig. 3 (c-d), after 12 h treatment, the dense structure shifted to a loose structure. Figure 2c shows that parts of hydrochar are fused and adhered between the microspheres at 250 ℃ after 12 h reaction time. The fragments and porosity of hydrochar increase due to gas emissions during devolatilization, and chemical bonds were broken. In Fig. 2d and S3d the degree of cellulose decomposition was more evident because the content of fixed carbon of cellulose-derived hydrochar is less than that of wood-derived hydrochar. Besides, the temperature can influence samples' structure by changing the properties of water, which easily permeates into the porous structure of hydrochars.

3.3 Chemical characterization

The elemental analysis of samples is shown in Table 2. Cellulose- and wood-derived hydrochars have a higher weight percentage of carbon and lower weight percentage of hydrogen and oxygen than their original substrates.

Table 2: The elemental analysis and atomic ratio of raw biomass and hydrochars.

	Elemental analysis			**atomic ratio**	
Samples	C (wt %)	H (wt %)	Oa (wt %)	H/C	O/C
Cellulose	39.3	6.61	54.09	1.98	1.03
C-200-6	41.60	6.03	52.37	1.74	0.94
C-250-6	62.48	4.79	32.73	0.92	0.39
C-250-12	63.30	4.50	32.20	0.85	0.38
Wood	46.4	6.05	47.55	3.86	3.86
W-200-6	57.80	5.92	36.28	1.23	0.47
W-250-6	70.80	5.01	24.19	0.85	0.26
W-250-12	71.90	4.93	23.17	0.83	0.24
a: The amount of oxygen was calculated according to O (wt %) = 100-C (wt %) -H (wt %)					

Higher HTC reaction temperature and longer reaction time can further increase the weight percentage of carbon and reduce hydrogen and oxygen weight. Normally, the H/C and O/C ratios were considered as indicators for the degree of carbonization of hydrochars. The H/C atomic ratios are 1.74 (200°C 6 h), 0.92 (250°C 6 h), 0.85 (250°C 12 h) for cellulose-derived hydrochar, and 1.23 (200°C 6 h), 0.85 (250°C 6 h) and 0.23 (250°C 12 h) for wood-derived hydrochar. The O/C atomic ratios are 0.94 (200°C 6 h), 0.39 (250°C 6 h) and 0.38 (250°C 12 h) for cellulose-derived hydrochar, and 0.47 (200°C 6 h), 0.26 (250°C 6 h), 0.24 (250°C 12 h) for wood-derived hydrochar. The higher temperature and longer reaction can decrease the H/C and O/C ratios. The reduction of H/C means more condensed aromatic structures were produced due to aromatization as fundamental components of hydrochar. Aromatization also improves the stability of

hydrochar in wood-derived hydrochar. The Decarboxylation process causes the reduction of the O/C by removing water from the raw materials without changing any chemical composition and produce CO2, and CO [40, 43][43].

A Van Krevelen diagram is shown in Fig. 4. As a kind of low-rank coal, the atomic ratios of lignite are 0.8–1.3 (H/C) and 0.2–0.38 (O/C) [41], and the atomic ratio of synthetic hydrochars under 250°C 6 h or 12 h is almost identical to that of lignite.

The results of the FTIR measurements were shown in Fig. 5. The band at 3000–3700 cm^{-1} is assigned to the O-H stretching vibrations of hydroxyl or carboxyl groups [44]. Due to the dehydration reaction, the peak of O-H becomes weak with increasing HTC temperature. Furthermore, it was reported that O-containing functional groups could absorb heavy metal ions (Kang et al., 2012; Liu and Zhang, 2009).

The band at 2800–3000 cm-1 is assigned to the stretching vibrations of aliphatic C-H, indicating an aliphatic structure [45]. The unobvious curves ranging from 2800 to 3000 cm^{-1} are attributed to the asymmetric stretching vibration of $-CH_3$ (2955 cm^{-1}) and $-CH_2-$ (2922 cm^{-1}), symmetric vibration of $-CH_3$ (2871 cm^{-1}) and $-CH_2-$ (2850 cm^{-1}), and stretching vibration of -CH (2900 cm^{-1}) [46]. The C-H vibration at around 2920 and 2850 cm^{-1} is related to asymmetric and symmetric methylene stretching groups present in all the wood components [47]. The band at 1700 cm^{-1} refers to C = O vibrations [43], while C = O belongs to the carboxyl group or carbonyl group, owing to the dehydration of hydroxyl [10]. The peak at 1620 cm^{-1} is assigned to C = C vibrations of aromatic structures [48]. The peaks at 1120 – 1050 cm^{-1} refer to the C – O bond.

The results show the peaks of C-O, C = O, and C-H in both cellulose-and wood-derived hydrochars decreased when reaction temperature increasing. That is because more bonds (C-O, C = O, and C-H) breaks during hydrothermal treatment [10]. Gases such as CH_4, C_2H_6, and C_2H_4 release when these bonds break and lead to the reduction of H/C and O/C ratio of hrdrichar.

XPS analyzed the hydrocarbon and oxygen-containing functional groups of hydrochars, and the results are shown in Fig. 6. For cellulose-derived and wood-derived hydrochar, two main peaks of C (C1s) at around 285 eV and O (O1s) at about 530 eV are usually observed in the XPS spectroscope [49]. The peaks at 284.6 eV were attributed to CH_X and C-C/C = C, which belong to aliphatic/aromatic carbon groups. The peaks at 285.7 eV and 287.3 eV were contributed by hydroxyl groups (-COR) and carbonyl groups (C = O), respectively. The small peak observed at 289.2 eV can correspond to carboxylic groups, esters (-COOR). It was also shown in the XPS results that the oxygen-containing functional groups such as hydroxyl groups, carbonyl groups, and esters existed on the surface of hydrochar.

Fig. 7 is the results of the FTIR measurements indicate that types and positions of functional groups of hydrochars after adding heavy metals are almost the same as those of hydrochars without heavy metals. Also, the SEM images of cellulose-derived and wood-derived hydrochar with heavy metals has been taken and it does not show difference with the one without heavy metal.

The speciation behavior of gaseous zinc-containing species was detected in atmospheres at 1200°C by using MBMS and the results are shown in Figs. 8 and 9. No peaks are determined in Fig. 8 (a) and Fig. 9 (a). One possible reason is that this may imply the very low partial pressures of the species zinc and zinc compounds under the present conditions, which are already outside of the sensitivity range of the instrument. Another possible reason is that zinc ions and other ions in hydrochar form high temperature resistant compounds, such as silicate minerals under hydrothermal carbonization process.

Compare Figs. 8 (b) and 9 (b), 10 wt% zinc is used in hydrothermal carbonization process, there is an obvious peak of zinc. Possible reason is that part of the zinc ions has formed high temperature resistant compounds, and the remaining zinc ions are combined with functional groups. For example, when Zn(II) is introduced into the hydrothermal carbonization reaction, these metal ions can be sorbed by phenolic, carboxyl, ester, and alcohol groups on the surface of the precursor [50][51]. by ion exchange interaction, large amount of phenolic, carboxyl and alcohol groups which are active functional group formed on the surface of hydrochars. Due to higher amount of zinc used, in Fig. 8 (b) and 9 (b), both of them show the peaks of zinc species. pure Zn gaseous species include $^{64}Zn^{+}$, $^{68}Zn^{+}$.

The previous study found that the structure of benzoic acid which is adsorbed on (0001)-Zn decompose to benzene under 300 K [52] Therefore, it is supposed that the connection of Zn and carboxyl grounp would promote decarboxylation reaction during the hydrothermal process. Moreover, Vohs et al. [52] reported that aromatic alcohols, benzyl alcohol, and phenol can form highly stable alkoxide species on the (0001)-Zn surface below 875 K. However, under high temperature, these organic functional groups are burned and zinc ions evaporate.

4. Conclusion

Cellulose and wood can be used to produce carbon-rich and valuable hydrochars via hydrothermal carbonization. The characteristics of hydrochars were influenced by reaction time and temperature. The results show that the temperature makes a great influence on the structural, chemical, and thermal characteristics of the hydrochars. With the increment of temperature, the crystalline region is broken down stepwise, the cellulose and wood are gradually converted into micro/nano carbon spheres. The hydrochars obtained at 200 ℃ are mainly composed of volatile matter. More prolonged reaction improves fixed carbon of wood-derived hydrochars form, but it has little impact on cellulose-derived hydrochars. At the same reaction, wood-derived hydrochar has more fixed carbon and condensed aromatic structures than cellulose-derived hydrochar. At 250 ℃, hydrochars obtained at 6 h and 12 h became stable, and their properties are similar to lignite-like fuel substances. Small amounts of heavy metals have no influence on the chemical and physical characteristics of hydrochar. More importantly, small amount of heavy metal species (Zn) may form high-temperature resistant compounds such as silicates, thereby the peaks of zinc are not determined. However, if large amounts of zinc are introduced, zinc can be bond to the surface of hydrochar by active groups which sheds light on the utilization of hyperaccumulator biomass from the remediation of heavy metal contaminated land.

Declarations

Funding: This work has been performed in the framework of the HotVeGas Project supported by Bundesministerium für Wirtschaft und Technologie (FKZ 0327773).

Conflicts of interest/Competing interests: The authors declare that there is no conflict of interest Not applicable.

Availability of data and material: All data generated or analyzed during this study are included in this published article.

Code availability: Not applicable.

References

1. Tekin K, Karagöz S, Bektaş S (2014) A review of hydrothermal biomass processing. Renew Sustain Energy Rev 40:673–687
2. Saxena RC, Adhikari DK, Goyal HB (2009) Biomass-based energy fuel through biochemical routes: A review. Renew Sustain energy Rev 13:167–178
3. Lehmann J (2007) A handful of carbon. Nature 447:143–144
4. Meyer S, Glaser B, Quicker P (2011) Technical, economical, and climate-related aspects of biochar production technologies: a literature review. Environ Sci Technol 45:9473–9483
5. Wang T, Zhai Y, Zhu Y et al (2018) A review of the hydrothermal carbonization of biomass waste for hydrochar formation: Process conditions, fundamentals, and physicochemical properties. Renew Sustain Energy Rev 90:223–247
6. Zhao P, Shen Y, Ge S et al (2014) Clean solid biofuel production from high moisture content waste biomass employing hydrothermal treatment. Appl Energy 131:345–367
7. Kwietniewska E, Tys J (2014) Process characteristics, inhibition factors and methane yields of anaerobic digestion process, with particular focus on microalgal biomass fermentation. Renew Sustain Energy Rev 34:491–500
8. Liu F, Yu R, Ji X, Guo M (2018) Hydrothermal carbonization of holocellulose into hydrochar: structural, chemical characteristics, and combustion behavior. Bioresour Technol 263:508–516
9. Nizamuddin S, Baloch HA, Griffin GJ et al (2017) An overview of effect of process parameters on hydrothermal carbonization of biomass. Renew Sustain Energy Rev 73:1289–1299
10. Kang S, Li X, Fan J, Chang J (2012) Characterization of hydrochars produced by hydrothermal carbonization of lignin, cellulose, D-xylose, and wood meal. Ind Eng Chem Res 51:9023–9031
11. Wang Q, Li H, Chen L, Huang X (2001) Monodispersed hard carbon spherules with uniform nanopores. Carbon N Y 39:2211–2214
12. Hu B, Wang K, Wu L et al (2010) Engineering carbon materials from the hydrothermal carbonization process of biomass. Adv Mater 22:813–828

13. Sharma HB, Sarmah AK, Dubey B (2020) Hydrothermal carbonization of renewable waste biomass for solid biofuel production: A discussion on process mechanism, the influence of process parameters, environmental performance and fuel properties of hydrochar. Renew Sustain Energy Rev 123:109761
14. Ischia G, Fiori L (2020) Hydrothermal Carbonization of Organic Waste and Biomass: A Review on Process, Reactor, and Plant Modeling. Waste and Biomass Valorization. https://doi.org/10.1007/s12649-020-01255-3
15. Bergius F (1928) Beiträge zur Theorie der Kohleentstehung. Naturwissenschaften 16:1–10
16. Berl E, Schmidt A (1928) Über das Verhalten der Cellulose bei der Druckerhitzung mit Wasser. Justus Liebigs Ann Chem 461:192–220
17. Berl E, Schmidt A, Koch H (1932) Über die entstehung der kohlen. Angew Chemie 45:517–519
18. Berl E, Schmidt A (1932) Über die entstehung der kohlen. II. Die inkohlung von cellulose und lignin in neutralem medium. Justus Liebigs Ann Chem 493:97–123
19. Berl E, Schmidt A (1932) Über die Entstehung der Kohlen. III. Die Inkohlung von Harzen und Wachsen in neutralem Medium. Justus Liebigs Ann Chem 493:124–135
20. Bode H (1932) Die Inkohlung eine Druckverschwelung? Angew Chemie 45:388–390
21. Cohen AD, Bailey AM (1997) Petrographic changes induced by artificial coalification of peat: comparison of two planar facies (Rhizophora and Cladium) from the Everglades-mangrove complex of Florida and a domed facies (Cyrilla) from the Okefenokee Swamp of Georgia. Int J Coal Geol 34:163–194
22. Davis A, Spackman W (1964) Role of cellulosic + lignitic components of wood in artificial coalification. Fuel 43:215
23. Erdmann E (1924) Der genetische Zusammenhang von Braunkohle und Steinkohle auf Grund neuer Versuche. Brennstoff-Chemie B 5:177–186
24. Hwang I-H, Aoyama H, Matsuto T et al (2012) Recovery of solid fuel from municipal solid waste by hydrothermal treatment using subcritical water. Waste Manag 32:410–416
25. Berge ND, Ro KS, Mao J et al (2011) Hydrothermal carbonization of municipal waste streams. Environ Sci Technol 45:5696–5703
26. Li H, Wang S, Yuan X et al (2018) The effects of temperature and color value on hydrochars' properties in hydrothermal carbonization. Bioresour Technol 249:574–581
27. Lu X, Pellechia PJ, Flora JRV, Berge ND (2013) Influence of reaction time and temperature on product formation and characteristics associated with the hydrothermal carbonization of cellulose. Bioresour Technol 138:180–190
28. Reza MT, Rottler E, Herklotz L, Wirth B (2015) Hydrothermal carbonization (HTC) of wheat straw: Influence of feedwater pH prepared by acetic acid and potassium hydroxide. Bioresour Technol 182:336–344

29. Yan W, Perez S, Sheng K (2017) Upgrading fuel quality of moso bamboo via low temperature thermochemical treatments: dry torrefaction and hydrothermal carbonization. Fuel 196:473–480
30. Oliveira I, Blöhse D, Ramke H-G (2013) Hydrothermal carbonization of agricultural residues. Bioresour Technol 142:138–146
31. Peng C, Zhai Y, Zhu Y et al (2016) Production of char from sewage sludge employing hydrothermal carbonization: char properties, combustion behavior and thermal characteristics. Fuel 176:110–118
32. Jin Y, Lu L, Ma X et al (2013) Effects of blending hydrothermally treated municipal solid waste with coal on co-combustion characteristics in a lab-scale fluidized bed reactor. Appl Energy 102:563–570
33. Gil-Lalaguna N, Sánchez JL, Murillo MB et al (2014) Energetic assessment of air-steam gasification of sewage sludge and of the integration of sewage sludge pyrolysis and air-steam gasification of char. Energy 76:652–662. https://doi.org/https://doi.org/10.1016/j.energy.2014.08.061
34. Hoekman SK, Broch A, Robbins C et al (2013) Hydrothermal carbonization (HTC) of selected woody and herbaceous biomass feedstocks. Biomass Convers Biorefinery 3:113–126. https://doi.org/10.1007/s13399-012-0066-y
35. Simsir H, Eltugral N, Karagoz S (2017) Hydrothermal carbonization for the preparation of hydrochars from glucose, cellulose, chitin, chitosan and wood chips via low-temperature and their characterization. Bioresour Technol 246:82–87. https://doi.org/10.1016/j.biortech.2017.07.018
36. Lin Y, Ge Y, Xiao H et al (2020) Investigation of hydrothermal co-carbonization of waste textile with waste wood, waste paper and waste food from typical municipal solid wastes. Energy 210:118606. https://doi.org/10.1016/j.energy.2020.118606
37. Volpe M, Messineo A, Mäkelä M et al (2020) Reactivity of cellulose during hydrothermal carbonization of lignocellulosic biomass. Fuel Process Technol 206:106456. https://doi.org/10.1016/j.fuproc.2020.106456
38. Adolfsson KH, Yadav N, Hakkarainen M (2020) Cellulose-derived hydrothermally carbonized materials and their emerging applications. Curr Opin Green Sustain Chem 23:18–24. https://doi.org/10.1016/j.cogsc.2020.03.008
39. Kalderis D, Kotti MS, Méndez A, Gascó G (2014) Characterization of hydrochars produced by hydrothermal carbonization of rice husk. Solid Earth 5:477
40. Xiao L-P, Shi Z-J, Xu F, Sun R-C (2012) Hydrothermal carbonization of lignocellulosic biomass. Bioresour Technol 118:619–623
41. He C, Giannis A, Wang J-Y (2013) Conversion of sewage sludge to clean solid fuel using hydrothermal carbonization: hydrochar fuel characteristics and combustion behavior. Appl Energy 111:257–266
42. Gao Y, Wang X-H, Yang H-P, Chen H-P (2012) Characterization of products from hydrothermal treatments of cellulose. Energy 42:457–465
43. Liu F, Guo M (2015) Comparison of the characteristics of hydrothermal carbons derived from holocellulose and crude biomass. J Mater Sci 50:1624–1631

44. Sevilla M, Maciá-Agulló JA, Fuertes AB (2011) Hydrothermal carbonization of biomass as a route for the sequestration of CO2: Chemical and structural properties of the carbonized products. Biomass Bioenergy 35:3152–3159
45. Sevilla M, Fuertes AB (2009) The production of carbon materials by hydrothermal carbonization of cellulose. Carbon N Y 47:2281–2289
46. Ibarra JV, Miranda JL (1996) Detection of weathering in stockpiled coals by Fourier transform infrared spectroscopy. Vib Spectrosc 10:311–318
47. Poletto M, Zattera AJ, Santana RMC (2012) Structural differences between wood species: evidence from chemical composition, FTIR spectroscopy, and thermogravimetric analysis. J Appl Polym Sci 126:E337–E344
48. Sun X, Li Y (2004) Colloidal carbon spheres and their core/shell structures with noble-metal nanoparticles. Angew Chemie 116:607–611
49. Manyà JJ (2012) Pyrolysis for biochar purposes: a review to establish current knowledge gaps and research needs. Environ Sci Technol 46:7939–7954
50. Cao X, Ma L, Gao B, Harris W (2009) Dairy-manure derived biochar effectively sorbs lead and atrazine. Environ Sci Technol 43:3285–3291
51. Betts AR, Chen N, Hamilton JG, Peak D (2013) Rates and mechanisms of Zn2 + adsorption on a meat and bonemeal biochar. Environ Sci Technol 47:14350–14357
52. Xu S, Adhikari D, Huang R et al (2016) Biochar-facilitated microbial reduction of hematite. Environ Sci Technol 50:2389–2395

Figures

Figure 1

TG and DTG images of different hydrochars: a) c-hydrochar 250 ℃ 12 h, b) c-hydrochar 250 ℃ 6 h, c) c-hydrochar 200 ℃ 6 h, d) w-hydrochar 250 ℃ 12 h, e) w-hydrochar 250 ℃ 6 h, f) c-hydrochar 200 ℃ 6 h.

Figure 2

SEM images of different c-hydrochars: a) 200 ℃ 6 h, b) 250 ℃ 6 h, c-d) 250 ℃ 12 h.

Figure 3

SEM images of different w-hydrochars: a) 200 ℃ 6 h, b) 250 ℃ 6 h, c-d) 250 ℃ 12 h.

Figure 4

Van Krevelen diagram of cellulose- and wood-derived hydrochar from hydrothermal treatment.

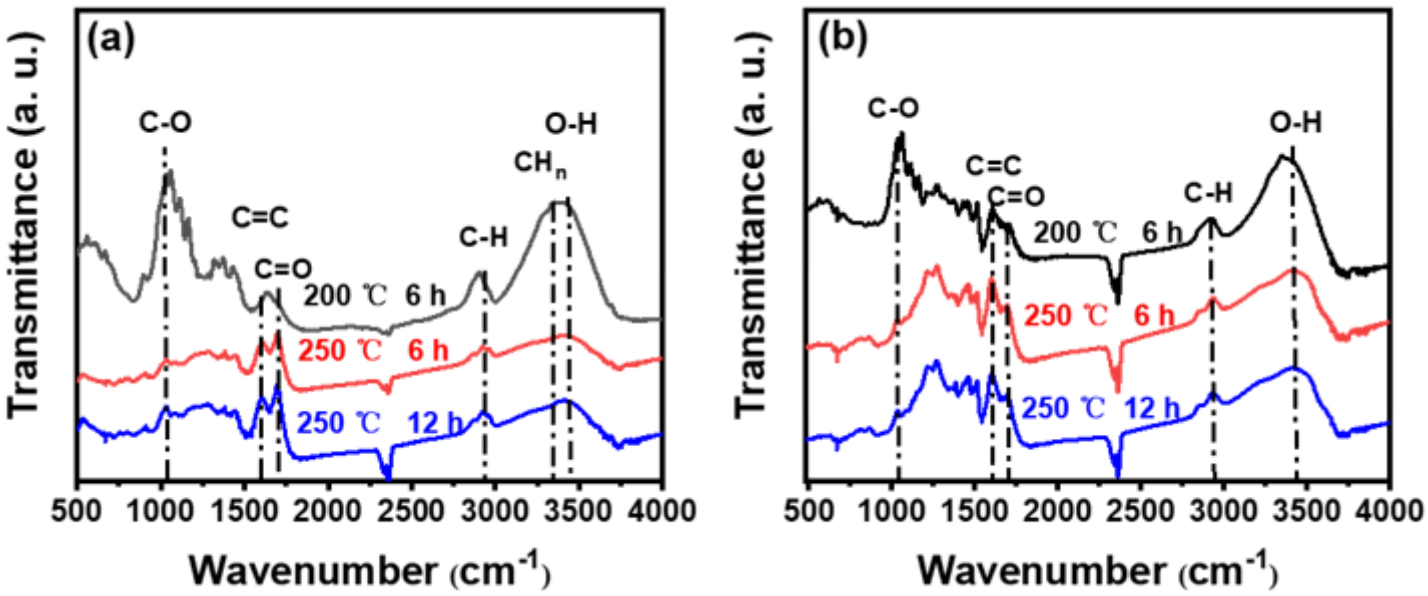

Figure 5

FTIR spectra of hydrochars: a) HTC of celluose, b) HTC of wood.

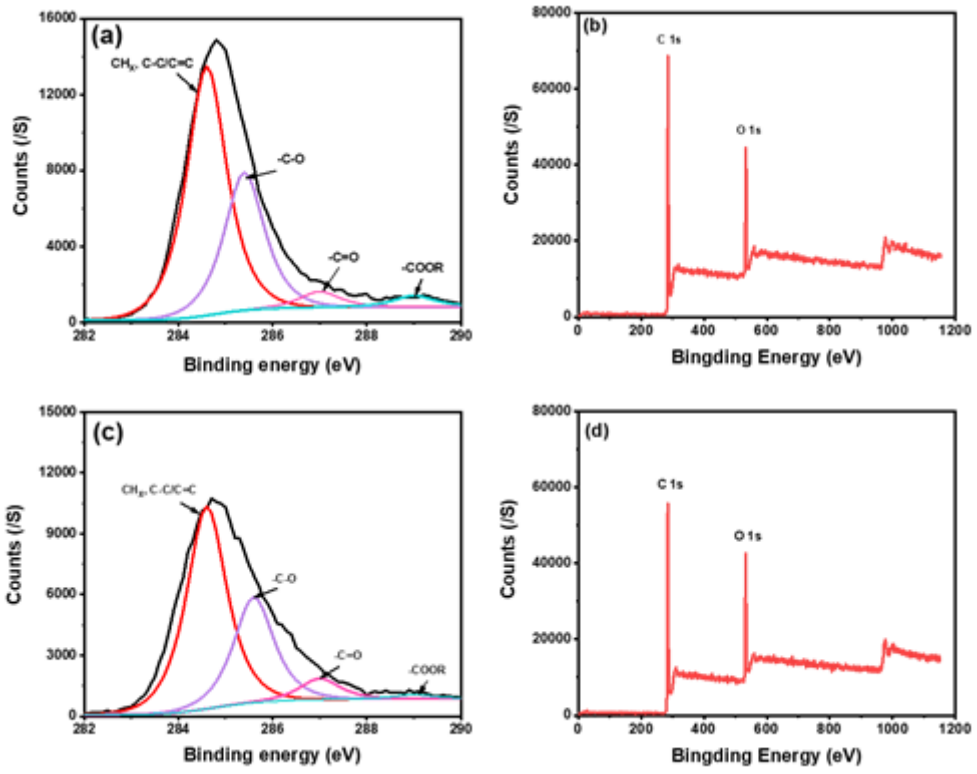

Figure 6

XPS spectrum of hydrochars: a-b) c-hydrochar, c-d) w-hydrochar at 250 °C for 6 h.

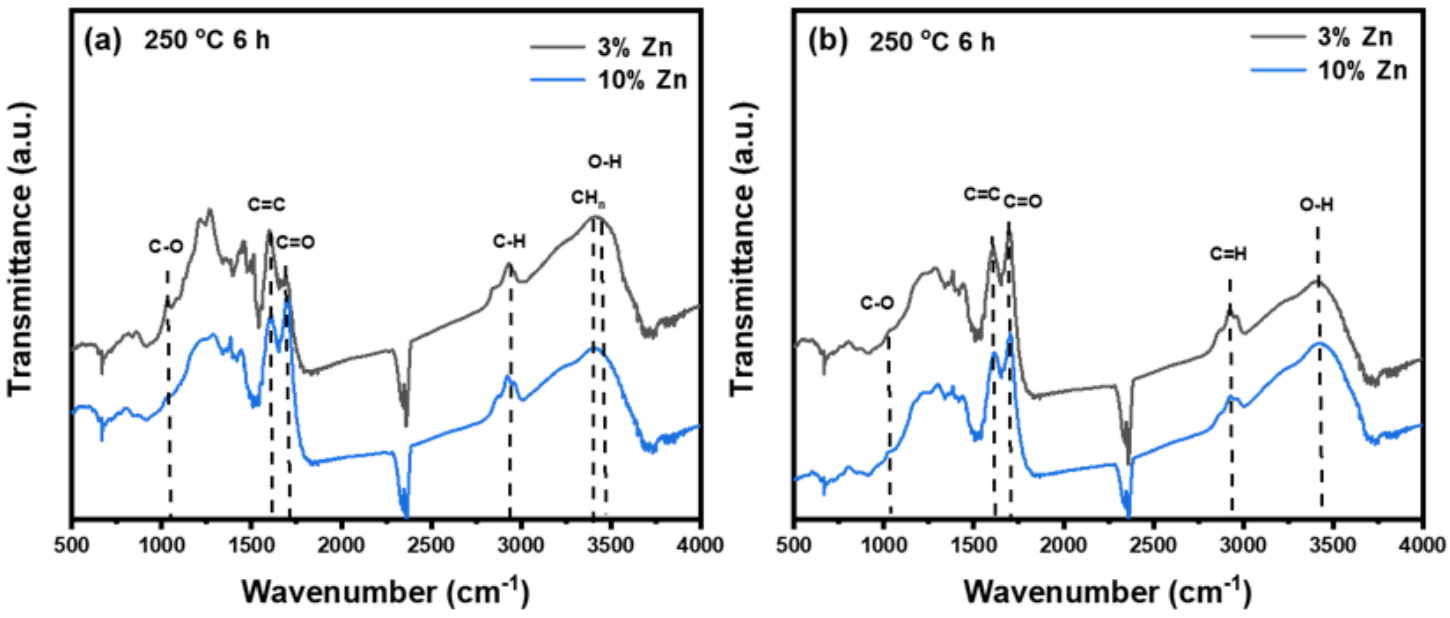

Figure 7

FTIR spectra of hydrochars with heavy metals: a) HTC of cellulose with 3% and 10% zinc, b) HTC of wood with 3% and 10% zinc

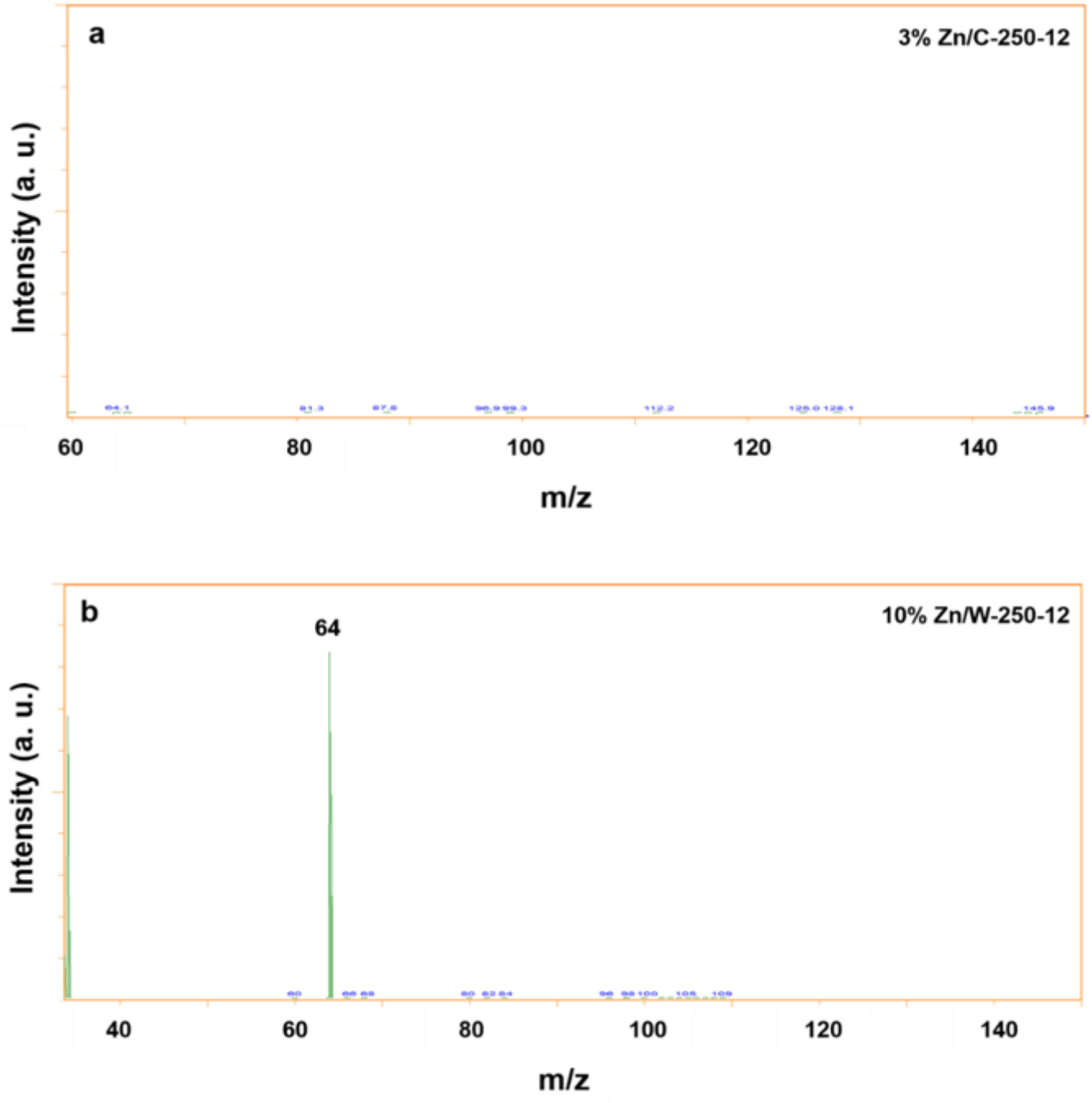

Figure 8

Exemplary MBMS images of gaseous zinc in the cellulose-derived hydrochar

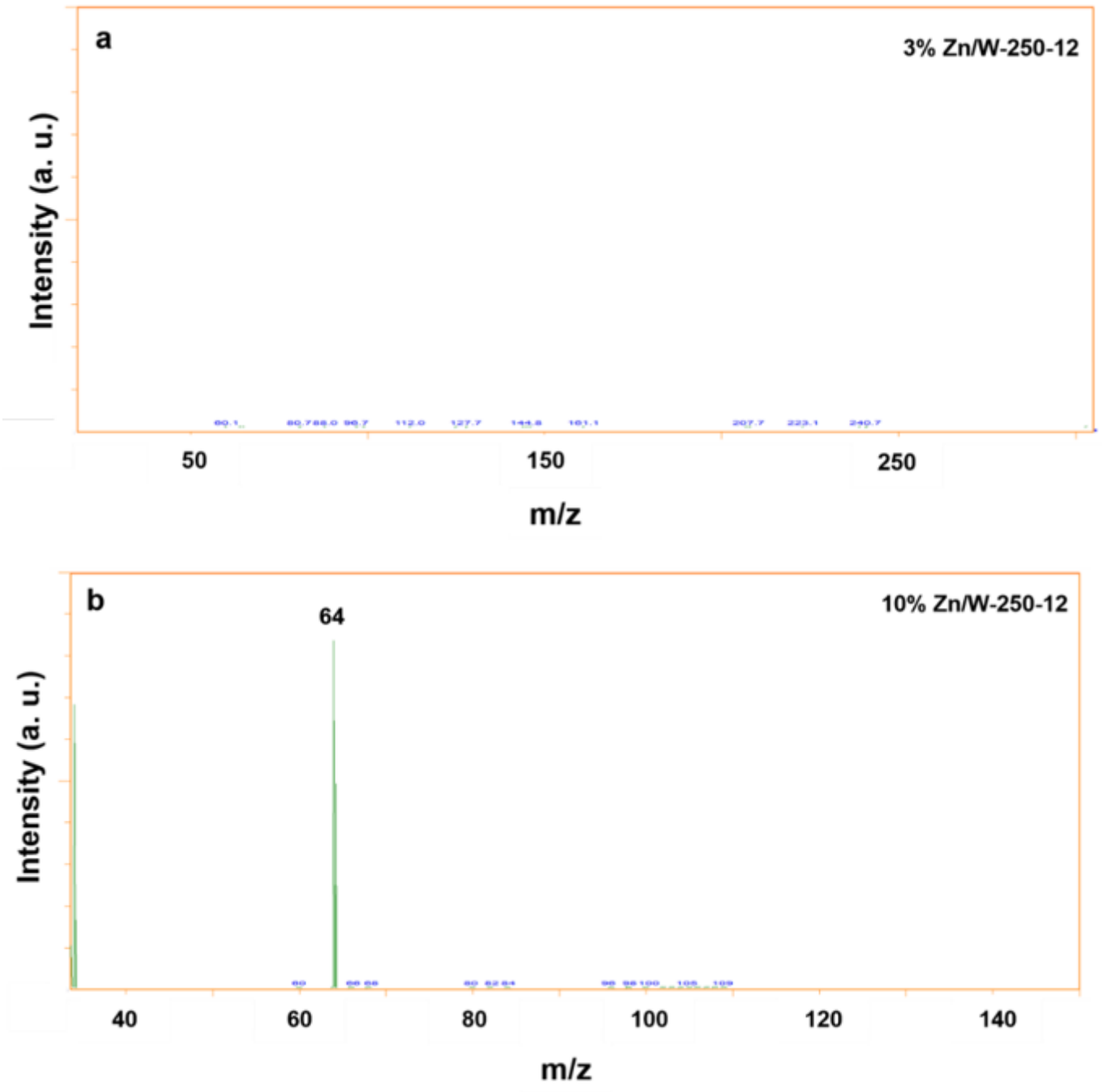

Figure 9

Exemplary MBMS images of gaseous zinc in the wood-derived hydrochar